

Salient Object Detection for Images Taken by People With Vision Impairments

Jarek Reynolds*, Chandra Kanth Nagesh*, and Danna Gurari

* denotes equal contribution
University of Colorado Boulder

Abstract

Salient object detection is the task of producing a binary mask for an image that deciphers which pixels belong to the foreground object versus background. We introduce a new salient object detection dataset using images taken by people who are visually impaired who were seeking to better understand their surroundings, which we call VizWiz-SalientObject. Compared to seven existing datasets, VizWiz-SalientObject is the largest (i.e., 32,000 human-annotated images) and contains unique characteristics including a higher prevalence of text in the salient objects (i.e., in 68% of images) and salient objects that occupy a larger ratio of the images (i.e., on average, $\sim 50\%$ coverage). We benchmarked seven modern salient object detection methods on our dataset and found they struggle most with images featuring salient objects that are large, have less complex boundaries, and lack text as well as for lower quality images. We invite the broader community to work on our new dataset challenge by publicly sharing the dataset at <https://vizwiz.org/tasks-and-datasets/salient-object>.

1. Introduction

Locating the most prominent foreground object in an image is a core computer vision problem, often referred to as salient object detection (as well as salient object segmentation and foreground object detection/segmentation) [8, 12, 32, 40]. This work is motivated by the desire to have salient object detection models work well for images taken by people who are blind or with low vision¹ (i.e., people with vision impairments). Such a feature could offer several benefits to this community. For example, it could contribute to privacy-preservation for photographers who rely on visual assistance technologies to learn about objects in their daily lives, using mobile phone applications such as Microsoft’s Seeing AI, Google Lookout, and TapTapSee.²

¹For people with low vision, solutions do not exist to correct their vision (e.g., by wearing glasses, surgery).

²Many companies record submitted data as evidence that potentially could be needed for legal reasons.

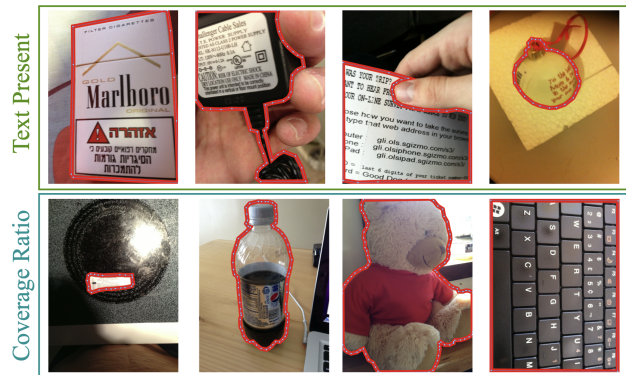


Figure 1. Example images demonstrating unique features of our new VizWiz-SalientObject dataset when compared to other datasets. The salient objects commonly contain text and occupy a larger portion of the image (i.e., high coverage).

All content except the foreground content of interest could be obfuscated, which is important since private information is often inadvertently captured in the background of images taken by these photographers [24]. Additionally, localization of the foreground object would empower low vision users to rapidly magnify content of interest and also enable quick inspection of smaller details [21, 39].

Many salient object detection datasets have been created to enable progress in algorithm development [7, 8, 22, 42]. A limitation of existing datasets is they are typically built using high-quality images collected from photo-sharing websites on the Internet. As we will show in Section 3.2, such images commonly lack many characteristics that can be observed in real-world settings, especially for visual media taken by visually impaired photographers who are trying to learn about the content they photograph [24], often photographing distinct types of content such as objects showing text [25], and cannot verify visual quality [13].

To fill this gap, we introduce a new salient object detection dataset based on images captured in an authentic use case where visually impaired photographers shared their images to solicit assistance in learning about the visual content. We created this dataset by crowdsourcing the collec-

tion of salient object annotations for nearly 40,000 images taken from the VizWiz-Captions dataset [25]. Examples of resulting annotated images are shown in Figure 1. After applying quality control filtration steps, our final dataset consists of 32,000 annotated images. We call our dataset VizWiz-SalientObject (or VizWiz-SO). We conduct a detailed analysis revealing how this new dataset relates to existing datasets. When comparing our salient objects to the visual evidence needed to answer questions the photographers asked about their images (i.e., taken from the VizWiz-VQA-Grounding dataset [11]), we observe that over half the time the necessary visual evidence is the salient object. When comparing our dataset to seven existing datasets, we observe VizWiz-SalientObject is the largest (i.e., 32,000 human-annotated images) and is unique in its higher prevalence of text in the salient objects (i.e., in 68% of images) as well as salient objects occupying a larger ratio of the images (i.e., on average, $\sim 50\%$).

We also benchmark modern salient object detection algorithms on our new dataset to uncover open challenges for the research community. Experiments with seven algorithms reveal that they struggle most for images with salient objects that are large, have less complex boundaries, and lack text as well as for lower quality images. To facilitate progress on these challenging problems, upon publication, we will publicly-share the dataset and an evaluation server with leaderboard at the following link: <https://vizwiz.org/tasks-and-datasets/salient-object>.

In summary, our new dataset supports the development of more generalized algorithms that not only address the interests of people with vision impairments but also can benefit related applications that encounter similar real world challenges observed in our dataset. Relevant applications include robotics, lifelogging, and privacy protection.

2. Related Work

Salient Object Detection Datasets. Over the past couple of decades, many datasets were introduced to facilitate improving the design of algorithms that address salient object detection problems. Several survey papers provide comprehensive characterizations of the tens of datasets designed for this task [7, 8, 22, 42]. A common observation is that datasets were artificially constructed around high-quality images which often feature salient objects in the center of the images with a high contrast against the background. This is a mismatch from many real-world settings, especially for visual media taken by visually impaired photographers who often photograph distinct types of content, such as objects showing text [25], with the aim to learn about that content. We introduce the first salient object detection dataset based on images taken by visually impaired people in an authentic use case where they were trying to learn about their visual surroundings. Compared to seven

modern datasets, our dataset is larger, has a high prevalence of salient objects containing textual information, and shows objects that occupy larger portions of the images.

Salient Object Detection Algorithms. Researchers have designed novel algorithms to automatically perform salient object detection for over 20 years, with the status quo since 2015 being that state-of-the-art methods employ neural networks trained on large-scale annotated datasets. Several survey papers provide comprehensive characterizations of the hundreds of algorithms for this task [7, 8, 22, 42]. While convolutional neural network (CNN) based models became the mainstream method [1, 33, 43] in 2015, transformer based models [30, 44] have become the mainstream approach over the past few years. To assess how well modern methods perform on our new dataset, we benchmark seven modern methods. We observe that existing methods fall below human performance and struggle most for salient objects that lack text and occupy a larger ratio of the image.

Visual Assistance Technologies. Visually impaired people can share their visual media (images and videos) with various technologies [3, 4, 6, 14, 18, 27, 32, 40] in order to receive assistance for daily tasks such as deciding what to eat, wear, and buy [10, 24]. The widespread impact of such technologies for real users is exemplified by reports from some of these companies that the technologies have 10s to 100s of thousands of users who have submitted millions of assistance requests [5, 9, 14, 17]. The most common reported goal for using such technologies is to learn about a (salient) object [9, 10, 23, 28, 47]. Given this common use case, salient object detection models could help for privacy preservation. Specifically, images (or video frames) could be edited before being shared with companies, by obfuscating the background, in order to reduce inadvertent disclosures of private content that often appears in the background of images taken by visually impaired photographers [24].

3. VizWiz-SalientObject Dataset

We now introduce our new salient object detection dataset, we call VizWiz-SalientObject (VizWiz-SO).

3.1. Dataset Creation

Image Source. We focus on images taken by visually impaired people who shared them in an authentic use case where they were soliciting visual assistance. Specifically, we leverage the 39,181 labeled images from the VizWiz-Captions dataset, each of which is paired with five crowd-sourced captions [25]. Observing that images from these photographers can have severe quality issues resulting in no detectable salient object (e.g., extreme blur or inadequate illumination), we did not use the images which were captioned as follows by at least four of the five crowdworkers:

“Quality issues are too severe to recognize visual content.” We also did not use the small images (i.e., both the height and width were less than 300 pixels) because of the challenges of collecting precise annotations for such images. This left us with 37,120 images for our annotation task.

Task Design. Our task interface for segmenting salient objects begins with a comprehensive instruction set at the top detailing both how to navigate the interface and how to complete challenging annotation scenarios. Next, it shows an image alongside two preliminary questions for verifying there is a single, unambiguous foreground object. The first question asks “Is the image showing a screenshot?” If the answer is “yes”, we conclude the image lacks a salient object. Next, we ask the more general, direct question of “Is there a single unambiguous foreground object?” An annotator is only prompted to segment the foreground object for images deemed by these preliminary questions to show a single, unambiguous foreground object.

To demarcate the boundary of the salient object, the interface collects a series of points that are connected into polygon(s). When segmenting the salient object, the annotator is required to remove any *holes* (e.g., donut) as well as capture all object parts when *occlusions* break a salient object into more than one polygon (e.g., hand obfuscates a pencil into two parts). The annotator also has an option to select a button indicating that the salient object occupies the full image. We provide more details about the task interface as well as a screenshot of it in the Supplementary Materials.

Annotation Collection. We leveraged the benefits of an around-the-clock distributed workforce by crowdsourcing annotations via Amazon’s crowdsourcing marketplace, Amazon Mechanical Turk (AMT).

Although AMT can support our large-scale annotation needs, it brings concerns about annotation quality due to the anonymous nature of the crowdsourced workforce. Consequently, we implemented several measures to ensure the collection of high-quality annotations, as summarized below. First, we restricted who were potential candidates for our task. We only accepted workers who had at least a 98% acceptance rate while having completed at least 500 Human Intelligence Tasks (HITs) on AMT. Moreover, to encourage understanding of our initial and ongoing task instructions, we opted for crowdworkers only from the United States since that provided us confidence that they have English-language proficiency. In addition, we also required crowdworkers to pass a qualification assessment covering five challenging annotation scenarios documented in our instructions. The qualification images feature foreground objects consisting of complex boundaries, holes within the object, and occlusions obfuscating portions of the foreground object. Consequently, the task required crowdworkers to

demonstrate an understanding of how to generate multiple polygons, annotate holes, handle occlusions, and draw complex boundaries.

We employed 40 AMT crowdworkers who completed our qualification task to complete annotations of all images. For each of the 37,120 images, we collected two annotations from the crowdworkers.³ During annotation collection, we monitored ongoing quality by tracking each worker’s performance with respect to their frequency of indicating the presence of full-screen annotations or no prominent foreground object as well as the level of detail they provided in their segmentations (e.g., high prevalence of triangles). Cumulatively, the crowdworkers took 1,290 annotation hours over 11 days to complete annotating the 37,120 images.

Annotation Post-Processing. We next analyzed the redundant annotations per image to determine how to use each annotated image in the final dataset. First, we removed 3,662 images for which workers agreed there was no single, unambiguous salient object, which occurred when both annotators either answered “Yes” to “Is the image a screenshot?” or “No” to “Is there a single most prominent foreground object?” Next, we manually inspected 7,443 images for which workers disagreed on the answers to either of the two preliminary questions and determined whether there is indeed a single, unambiguous object. Finally, with all images deemed to have a single, unambiguous salient object, we determined which annotation to assign as ground truth. To assist in this process, we computed the intersection over union (IoU) score between the two segmentations for all images with two or more segmentations. With $\text{IoUs} \geq 0.90$, we deemed both annotations high quality and randomly selected one as ground truth. For the remaining 2,951 images with $\text{IoUs} < 0.90$, we manually reviewed the annotations to decide whether one was correct or whether the image should be discarded due to foreground object ambiguity.

3.2. Dataset Analysis

We now characterize the VizWiz-SalientObject (VizWiz-SO) dataset and how it relates to existing datasets.

3.2.1 Salient Objects vs Answer Groundings for VQA

We first explore how the target content the photographers were asking about relates to an image’s salient object. To do so, we compare the annotations of the visual evidence needed to answer questions about the images, i.e., *answer groundings* provided in the VizWiz-VQA-Grounding dataset [11], to the annotations of the salient objects in our dataset. We first identified all annotated images that were in

³For a subset of images, we collected four annotations to support further analysis of human annotation performance, which we describe in the Supplementary Materials.

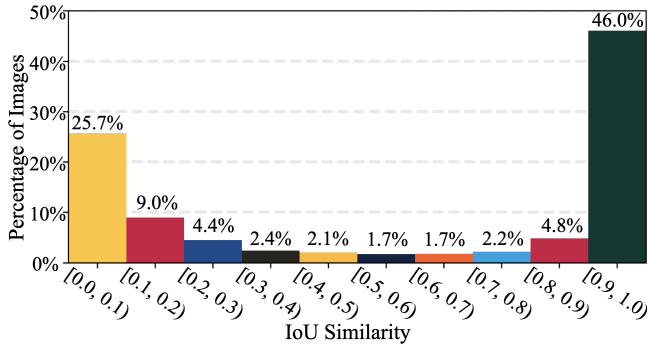


Figure 2. The histogram summarizes for 6,540 images the frequency of observing different levels of similarity between two segmentations per image, which show the salient object and the visual evidence needed to answer the photographer’s question respectively. These findings reveal that visually impaired photographers often want to learn about the salient objects in their images.

common across the two datasets, yielding a total of 6,540 images. For each image, we then measured the similarity between the answer grounding and salient object segmentations using the IoU metric. We visualize our results using a histogram where we categorize each image into one of ten interval bins starting with $\text{IoU}=[0.0, 0.1)$, incrementing in intervals of 0.1, and ending with $\text{IoU}=[0.9, 1.0)$. Results are shown in Figure 2.

We observe that about half of the images have a high similarity between the salient object and VQA answer grounding; e.g., 46% had an $\text{IoU} \geq 0.9$. This reveals that visually impaired photographers often are trying to learn about the salient object in their images when trying to get answers to their visual questions.

We also observe that roughly one quarter of the images have a very low similarity between the salient object and VQA answer grounding; i.e., 25.7% of images had an $\text{IoU} < 0.1$. We manually reviewed these 1,680 images with IoU s less than 0.1 to understand the reasons for this finding. We discovered that 95% (i.e., 1,599) of these images have a salient object featuring a full-screen or large region while the VQA answer grounding captures a small aspect of the salient object. Examples include expiration dates on food packages or the current page number of an open book. The remaining 5% (i.e., 81) of these images featured a VQA answer grounding unrelated to the salient object.

More generally, we observe that the IoU scores follow a U-shaped distribution with only a small portion of images having middling scores; e.g., 7.9% (i.e., 511) of images had an $\text{IoU} \geq 0.3$ and < 0.7 . Among these images, we found the salient object contained the VQA answer grounding region 100% of the time. There are two primary trends that led to these less common IoU scores. The first trend is that larger VQA answer grounding regions occur with smaller salient

objects. Examples include brands of cereal, types of soda, and denominations of currency. The second trend was for salient objects featuring holes. That is because the VizWiz-VQA-Grounding dataset did not account for holes in their annotation task. The absence of annotated holes in only one of the two segmentations led to lower IoU scores.

Altogether, these findings highlight that a valuable step for tackling many of this population’s VQA goals is to initially locate the salient object. That is because the answer will likely only be grounded in the salient object *or* the background rather than their intersection.

3.2.2 VizWiz-SO vs Existing Datasets

We next compare our dataset to seven datasets:

- *DUTS* [41]: the most commonly used dataset to train state-of-the-art algorithms (e.g., [1, 30, 33, 38, 43, 44]) due to its large size paired with diverse saliency challenges.
- *DUT-OMRON* [46]: consist of images showing multiple salient objects, often with complex backgrounds. This is a useful reference when considering extending our dataset to when photographs taken by visually impaired photographers showing multiple salient objects. We share our collected metadata indicating when this occurs to facilitate this line of future research.
- *ECSSD* [45]: consists of images featuring complex scenes that present textures and structures expected to be common in real-world salient object detection scenarios.
- *PASCAL-S* [29]: derived from PASCAL VOC’s [16] validation set, it is designed to facilitate salient object segmentation generalization on realistic images.
- *HRSOD* [48]: explicitly designed for salient object detection on high-resolution images; this is relevant for our real-world application since images taken by people with vision impairments often are relatively high resolution.
- *UHRSD* [44]: currently the largest ultra-high resolution salient object detection dataset, which is relevant to our work since images taken by people with vision impairments can be ultra high resolution.
- *DAVIS-S* [48]: derived from DAVIS [36], a densely annotated video segmentation dataset. This is relevant for our real-world application to analyze implications for video frames since visually impaired photographers often stream live video with their cameras when using visual assistance technologies [4, 18].

Of note, images in six of these datasets originate from the Internet on photo-sharing websites such as Flickr [29, 41, 44–46, 48], and so likely are high quality since they were deemed of sufficient quality to upload to the Internet.⁴

⁴The origins of the images for the final dataset is not reported [48].

	DAVIS-S [48]	PASCAL-S [29]	HR [48]	ECSSD [45]	DUT-O [46]	UH [44]	DUTS [41]	Ours
Images	92	850	2,010	1,000	5,168	5,920	15,572	32,000
Text	13%	24%	15%	15%	11%	19%	13%	68%
MR	22%	31%	25%	9%	17%	35%	19%	1%
Holes	82%	50%	62%	29%	28%	75%	41%	4%

Table 1. Characterization of our VizWiz-SO dataset and seven existing salient object detection datasets with respect to how many images are included (“Images”), the percentage of images that have text present in the salient objects (“Text”), the percentage of images that have salient objects consisting of more than one region (“MR”), and the percentage of images that have salient objects containing any holes (“Holes”). As shown, our dataset is distinct in that it contains more images, more salient objects with text present, more salient objects consisting of one region, and fewer salient objects containing holes. (HR=HRSOD; UH=UHRSD)

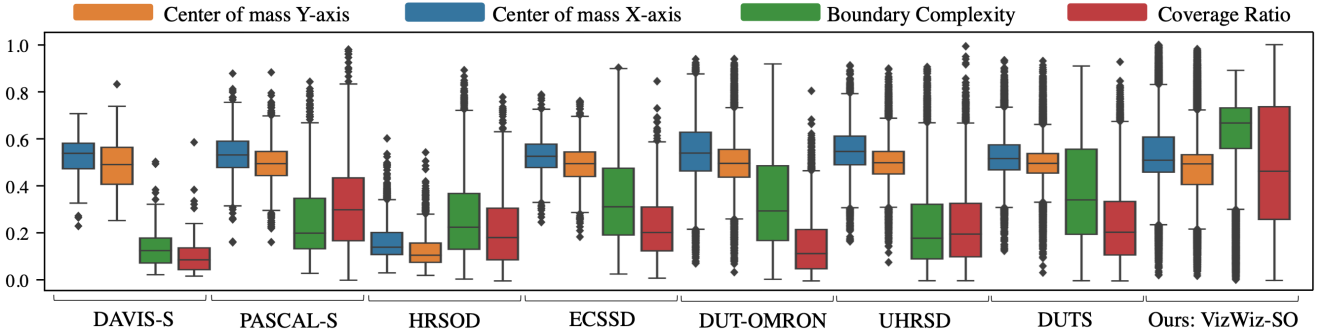


Figure 3. Summary statistics for ours and seven other datasets with respect to four measures. Each box reveals statistics about all salient objects in a particular dataset with the central mark capturing the median value, box edges the 25th and 75th percentile values, whiskers the most extreme data points not considered outliers, and individually plotted points the outliers. Our dataset is unique in that salient objects tend to have less complex boundaries, occupy larger portions of an image, and exhibit a greater diversity of sizes relative to the image.

For each salient object in every dataset, we characterize it in six ways. Three measures focus on detecting the presence versus absence of particular properties for the salient object. These are whether the salient object *contains text*⁵, *consists of multiple regions*⁶, or *contains any hole(s)*. The remaining three measures characterize the salient region itself. First, we identify the position of an object within an image by measuring its *center of mass* relative to the image coordinates, resulting in x and y coordinate values in the range between 0 to 1. Next, we characterize the object’s *boundary complexity* by computing its isoperimetric inequality, which is the ratio of the object’s area to the length of its perimeter. Values range from 0 to 1, with larger values indicating simpler boundaries that are less jagged/dented (e.g., a circle). Finally, to gauge the relative size of a salient object in the image, we compute its *coverage ratio*, meaning the fraction of all image pixels that are occupied by the salient object’s pixels.

We show summative statistics of our findings per dataset in Table 1 and Figure 3. In particular, in Table 1, we re-

⁵We obfuscate all image content but the salient object and then check whether Microsoft Azure’s OCR API returns text.

⁶Multiple regions means there are multiple separate polygons. This can occur either because multiple salient objects were annotated or because of occlusions that lead to more than one region for a single salient object.

port how many images are in each dataset paired with what percentage of those images have salient objects with text, multiple regions, and holes. In Figure 3, we visualize statistics summarizing the values for each dataset’s salient objects with respect to center of mass, boundary complexity, and coverage ratio using boxplots.

While our findings highlight that our VizWiz-SO dataset has many distinct characteristics, one commonality it has with most existing salient object detection datasets is that the salient objects typically occupy centered positions within an image. Specifically, in Figure 3, we observe this trend for all datasets except HRSOD. We found this somewhat surprising since visually impaired photographers cannot visually inspect their images to verify they are conforming to the common photographer’s bias of centering contents of interest they are trying to photograph. Yet, given our findings from Section 3.2.1 that photographers often are interested in learning about an image’s salient object, our findings suggest these photographers have skills in centering contents of interest in pictures they take.

A unique aspect of our VizWiz-SO dataset is that it features more salient objects with textual data. Specifically, 68% of salient objects in VizWiz-SO contain text while the dataset with the next highest prevalence of text, PASCAL-S [29], only has it for 24% of the images (Table 1). A gap of

this magnitude (i.e., 44 percentage points) suggests that our new dataset offers a considerable domain shift in the salient object detection problem space. We suspect part of this shift stems from the types of salient objects included, with many more daily objects such as products (e.g., food packages) included in our VizWiz-SO dataset.

Another unique aspect of VizWiz-SO is that far fewer images feature salient objects that consist of multiple regions; i.e., only 1% of images (Table 1). We suspect this distinction stems from our unique approach of adopting a rigorous annotation preprocessing step, where we require crowdworkers to verify images have one unambiguous salient object before allowing them to annotate images for use in our final dataset. Any remaining objects in our dataset with multiple regions are therefore highly likely a result of occlusions breaking a single salient object into multiple polygons, which evidently is incredibly rare.

VizWiz-SO is also unique due to the rarity in which salient objects contain holes; i.e., only observed for 4% of images (Table 1). From visual inspection, we suspect this finding reflects a domain shift in the types of content found in the datasets. For example, examples from other datasets of objects with holes include people riding bikes, people dancing, and animals in intricate poses. In contrast, in VizWiz-SO, objects with holes include retail packaging made to hang from hooks, pairs of scissors, and coffee mugs. We posit the lower prevalence of holes in VizWiz-SO stems from the fact that images originate from an authentic use case where photographers primarily photograph household and retail items, which naturally feature fewer holes.

A further distinction of our VizWiz-SO dataset is that the salient objects tend to have less complex boundaries (Figure 3). We suspect this is again because of a domain shift in the types of objects in our dataset, with many more human-made items, such as food packaging boxes and cans, that by design are typically more structured in shape.

A final distinction of salient objects in our VizWiz-SO is how much of the image they occupy (Figure 3). First, they tend to occupy a much larger amount of the image than observed in other datasets. Specifically, they on average occupy roughly half of all image pixels, with a mean coverage ratio of 0.5 and a median of 0.46. In contrast, the dataset with the next highest coverage ratio statistics is PASCAL-S [29], and over 75% of its images contain salient objects that occupy less than half of the image pixels. We attribute this distinction to the authentic use case of our dataset, where visually impaired photographers attempting to learn about the salient objects they are photographing seem to be taking zoomed-in or close-to-camera images of the content of interest. Another unique aspect of our salient objects, is that they exhibit a larger range of sizes, as shown by the gaps between the 25 and 75 percentile values of each box. For example, PASCAL-S features the next largest interquar-

tile range with a 23% gap (i.e., 19% to 42%). In contrast, the gap for VizWiz-SO is more than twice as large at 56% (i.e., 22% to 78%). Consequently, a unique challenge of our dataset for algorithms is that they no longer can assume a strong bias regarding a salient object’s relative size.

4. Algorithm Benchmarking

We benchmark modern salient object detection algorithms to show how they perform on our new dataset. We conducted all experiments on a Nvidia A100 GPU.

4.1. Experimental Design

Dataset Splits. We use the existing splits available for the VizWiz-Captions dataset [25], which translates to approximately a 60/20/20 training, validation and test split for our VizWiz-SO dataset. In particular, from the 32,000 annotated images, the number of images in each split respectively is 19,116, 6,105, and 6,779.

Evaluation Metrics. We evaluate each model with respect to five popular metrics for salient object detection models: Mean Absolute Error (MAE), Structure Measure (S_m), Mean F-Measure (F_m), Enhanced Alignment Measure (E_m), and Intersection over Union (IoU).

Algorithms. We benchmark the following seven methods from the past three years to assess the difficulty of our new dataset for modern salient object detection models:

- *Boundary Aware Segmentation Network (BASNet)* [38]: an appealing model for real-time applications like our target use case because it can achieve 70fps during inference time while achieving competitive performance (i.e., was a top-performer in 2019).
- *Fusion, Feedback and Focus Network (F3Net)* [43]: state-of-the-art performing model on five datasets in 2020.
- *U2 Network (U2Net)* [1]: an appealing model for real-world applications like our target use case because it has a very light footprint (4.7MB), and so is more suitable for resource-constrained devices such as smartphones. It achieved competitive performance in 2020.
- *Visual Saliency Transformer (VST)* [30]: achieved state-of-the-art performance in 2021, and is based purely on a transformer architecture.
- *Pyramidal Feature Shrinking Network (PFSNet)* [33]: achieved state-of-the-art performance on five datasets in 2021; it consists of a decoder that aims at using aggregated adjacent feature nodes hierarchically to avoid the problem of leaping feature fusion.
- *Pyramid Grafting Network (PGNet)* [44]: introduced in 2022, it is a one-stage framework based on a transformer

	HP	BASNet [38]	F3Net [43]	U2Net [1]	VST [30]	PFSNet [33]	PGNet [44]	DIS [37]	VST-FT	VST-S	
Attr.	Backbone	-	R-34	R-50	-	T2T-ViT	R-50	R-18+SWIN	U2Net	VST	ViT
	Training set	-	D	D	D	D	D	D+HR	DIS5K	D+VW	VW
	Input size	-	256 ²	352 ²	320 ²	224 ²	352 ²	224 ² , 1024 ²	1024 ²	224 ²	224 ²
	Size (MB)	-	333	98	4.7	171	120	280	169	171	171
VizWiz-SO	$MAE \downarrow$	0.02	0.28	0.28	0.26	0.17	0.32	0.21	0.36	0.19	0.21
	$S_m \uparrow$	0.92	0.59	0.55	0.61	0.65	0.48	0.62	0.46	0.64	0.63
	$F_m \uparrow$	0.96	0.77	0.74	0.80	0.83	0.70	0.79	0.61	0.74	0.72
	$E_m \uparrow$	0.97	0.64	0.65	0.65	0.76	0.60	0.74	0.55	0.77	0.70
	$IoU \uparrow$	0.94	0.62	0.53	0.63	0.73	0.48	0.67	0.49	0.70	0.69

Table 2. Analysis of existing algorithms that we benchmark on our VizWiz-SO dataset, including both off-the-shelf models (which are cited) as well as those fine-tuned (-FT) and trained from scratch (-S). We first report differentiating attributes between the algorithm architectures and then present the model performance with respect to five widely-used metrics. (HP=Human Performance; R=ResNet [26]; ViT=Vision Transformer [15]; Swin=Shifted window transformer [31]; D=DUTS-TR [41]; VW=VizWiz-SO; HR=HRSOD [48])

and CNN backbone that achieves state-of-the-art performance on five benchmark datasets. [41, 44, 46, 48].

- *Dichotomous Image Segmentation (DIS)* [37]: also introduced in 2022 as the state-of-the-art method for the DIS5K [37] dataset; it is designed for detecting salient object in high resolution images, which makes it relevant for our use case where many images coming from people with vision impairments are relatively high resolution.

We further characterize each model by identifying the backbone architecture used in the architecture, datasets used for training, image size used for training, and model footprint. These characteristics are reported in Table 2.

All models predict saliency maps that represent the brightness of certain pixels within the same spatial resolution as the input image; e.g., $\in [0, 1]$ or alternatively $\in [0, 255]$. The predictions generated by salient object detection models are converted into binary masks.

Humans. We also evaluate human performance to establish an upper bound for what we should strive for from automated methods. Since, we get two human annotations per image in our dataset, we calculate human performance by comparing the two annotations in cases where the IoU is greater than 0.90.

4.2. Performance for Off-The-Shelf Models

We first evaluate each of the algorithms as is in their original design. Results are shown in Table 2.

We observe that VST [30] is the top-performing model. Yet, it still falls short of human performance. For example, the gap in performance is 0.15 in terms of MAE, 0.211 in terms of IoU, 0.26 for S_m , and 0.2 for E_m . Consequently, this dataset offers a new challenging benchmark for the community.

A further observation is that the models perform poorly on the VizWiz-SO dataset in comparison to their performance on the original datasets for which they were benchmarked. For example the MAE and S_m performance observed by PGNet [44] on DUTS-TE is 0.028 and 0.912 respectively versus 0.2123 and 0.6233 respectively for our dataset. We hypothesize that part of the reason for this poor performance is that models trained and evaluated on other datasets are not able to learn how to generalize to the real-world challenges that arise for images taken by visually impaired photographers.

4.3. Performance When Training on VizWiz-SO

We next explore whether training the top-performing algorithm, VST [30], on our new dataset will lead to improved performance. To do so we analyze two additional models: (1) the pretrained VST [30] model fine-tuned on VizWiz-SO (VST-FT) and (2) the pretrained VST [30] algorithm trained from scratch on VizWiz-SO (VST-S). We use the default hyperparameters reported in the VST [30] paper for model training. Results are shown in Table 2.

We observe that both models, i.e., created by training from scratch and fine-tuning on our VizWiz-SO dataset, achieve *worse* results than the baseline of not training the algorithm on our dataset. This suggests that the training data used by algorithms is not the only culprit for what makes our new dataset challenging. Rather, our findings suggest that new algorithmic frameworks are also needed to achieve strong generalization performance on our new dataset.

4.4. Fine-grained Analysis

We next conduct fine-grained analysis to better isolate what makes our dataset challenging for modern algorithms. To do so, we divide our VizWiz-SO test set according to the following *four* factors, with the first three based on metadata collected in Section 3.2 to characterize our dataset:

		BASNet	F3Net	U2Net	VST	PFSNet	PGNet	DIS	VST-FT	VST-S
		[38]	[43]	[1]	[30]	[33]	[44]	[37]		
Text Presence	True	0.23	0.22	0.22	0.13	0.25	0.16	0.32	0.16	0.17
	False	0.35	0.38	0.32	0.24	0.42	0.29	0.40	0.24	0.26
Coverage	Small	0.06	0.16	0.07	0.11	0.16	0.12	0.10	0.09	0.11
	Medium	0.15	0.20	0.15	0.09	0.24	0.15	0.25	0.09	0.10
	Large	0.60	0.47	0.54	0.30	0.54	0.35	0.70	0.38	0.39
Complexity	High	0.15	0.21	0.15	0.12	0.24	0.16	0.21	0.11	0.12
	Low	0.38	0.34	0.35	0.21	0.38	0.25	0.48	0.26	0.27
Image Quality	Good	0.22	0.23	0.21	0.14	0.26	0.17	0.30	0.16	0.17
	Poor	0.44	0.43	0.41	0.27	0.47	0.34	0.50	0.30	0.31

Table 3. Fine-grained analysis of existing algorithms with respect to presence of text on the salient object (“Text Presence”), relative size of the salient object in the image (“Coverage”), relative complexity of the salient object’s boundary (“Complexity”), and image quality (“Image quality”). As shown the algorithms perform worse when there is salient objects lack text, occupy a large portion of the image, have less complex boundaries as well as when the image quality is poor.

- *Text Presence*: two groups based on whether text is present in the salient object.
- *Coverage Ratio (Coverage)*: three groups based on the 33rd and 66th quartile values in our dataset. All images with coverage ratio less than 0.32 has *small* coverage, between 0.32 and 0.62 has *medium* coverage, and greater than 0.62 has *large* coverage.
- *Boundary Complexity (Complexity)*: two groups by splitting them around the mean score for boundary complexity (i.e., 0.66) with *high* boundary complexity when the score is less than the mean and *low* boundary complexity otherwise.
- *Image Quality*: leveraging metadata from prior work [25], which indicates how many of the five crowdworkers indicated an image as insufficient quality to recognize the content, we split the images into groups with *good* quality being when none of the crowdworkers indicate insufficient quality and *poor* otherwise.

Due to space constraints, we only report results in the main paper with respect to the *Mean Absolute Error* [35]. Results for all benchmarked models are shown in Table 3.

In terms of text presence, we see that the models perform better when there is text present as opposed to when there is none. For example, the performance drops by 0.11 for the best performing model, VST. We suspect visual patterns that arise with text may serve as a valuable cue to models in locating salient objects.

Next, we see that as the coverage ratio of the salient objects increase, the models tend to perform worse. For instance, the best performing model, VST, has a performance dropoff of 0.19 when predicting images with small coverage ratios as opposed to large coverage ratios. We see an even greater performance dropoff from other models such as 0.60 for DIS. We suspect this performance gap arises in

part from the fact that existing datasets largely lack such large salient objects, which both could have affected what algorithms were designed to handle as well what they could learn from the data they observed.

Further observed trends are that performance drops for salient objects with lower boundary complexity and for poorer quality images. These are two additional factors that reflect domain shifts between our dataset and prior datasets that could have affected the design of algorithms as well what they could learn from the data training data.

5. Conclusions

We introduce the VizWiz-SalientObject dataset to encourage the community to design more generalized salient object detection models that can handle a larger range of challenges motivated by our authentic use case that also can occur in many real-world applications. We offer our experimental findings from benchmarking modern salient object detection algorithms as a valuable starting point for identifying valuable future research directions. To summarize, new models are needed to better handle salient objects that are large, have less complex boundaries, and lack text as well as work well in the presence of lower quality images.

We now close with a discussion of some ethical implications of our work. While we are motivated to better assist a population that is traditionally marginalized in society, we acknowledge our work can lead to potentially adverse social effects. Our concern is primarily centered on bad-actor behaviors intended to exploit the privacy, autonomy, and livelihoods of a population demographic inherently susceptible to such behavior. Bad actors could use our work to deceive visually impaired individuals in harmful ways, such as through fraud, scams, and other deceptive practices, by for example intercepting their visual media and replacing automatically detected salient objects with misinformation.

Acknowledgments. This project was supported in part by a National Science Foundation SaTC award (#2148080) and Amazon Mechanical Turk. We thank Leah Findlater and Yang Wang for contributing to this research idea.

References

- [1] U2-net: Going deeper with nested u-structure for salient object detection. *Pattern Recognition*, 106:107404, 2020. 2, 4, 6, 7, 8
- [2] Radhakrishna Achanta, Sheila Hemami, Francisco Estrada, and Sabine Süsstrunk. Frequency-tuned salient region detection. In *CVPR*, number CONF, pages 1597–1604, 2009. 13
- [3] Aipoly. Aipoly homepage. <https://www.aipoly.com/>, 2020. (Accessed on 01/08/2020). 2
- [4] Aira. Aira homepage. <https://aira.io/>, 2020. (Accessed on 01/08/2020). 2, 4
- [5] BeSpecular. BeSpecularPressKit. 2
- [6] BeSpecular. Bespecular. <https://www.bespecular.com/>, 2020. (Accessed on 01/08/2020). 2
- [7] Ali Borji, Ming-Ming Cheng, Qibin Hou, Huaizu Jiang, and Jia Li. Salient object detection: A survey. *Computational visual media*, pages 1–34, 2019. 1, 2
- [8] Ali Borji, Ming-Ming Cheng, Huaizu Jiang, and Jia Li. Salient object detection: A benchmark. *IEEE transactions on image processing*, 24(12):5706–5722, 2015. 1, 2
- [9] Erin Brady and Jeffrey P Bigham. Crowdsourcing accessibility: Human-powered access technologies. 2015. 2
- [10] Erin L Brady, Yu Zhong, Meredith Ringel Morris, and Jeffrey P Bigham. Investigating the appropriateness of social network question asking as a resource for blind users. In *Proceedings of the 2013 conference on Computer supported cooperative work*, pages 1225–1236. ACM, 2013. 2
- [11] Chongyan Chen, Samreen Anjum, and Danna Gurari. Grounding answers for visual questions asked by visually impaired people. *arXiv preprint arXiv:2202.01993*, 2022. 2, 3
- [12] Ming-Ming Cheng, Niloy J Mitra, Xiaolei Huang, Philip HS Torr, and Shi-Min Hu. Global contrast based salient region detection. *IEEE transactions on pattern analysis and machine intelligence*, 37(3):569–582, 2014. 1
- [13] Tai-Yin Chiu, Yinan Zhao, and Danna Gurari. Assessing image quality issues for real-world problems. In *Proceedings of the IEEE/CVF Conference on Computer Vision and Pattern Recognition*, pages 3646–3656, 2020. 1
- [14] Ned Desmond. Microsoft’s Seeing AI founder Saqib Shaikh is speaking at Sight Tech Global. 2
- [15] Alexey Dosovitskiy, Lucas Beyer, Alexander Kolesnikov, Dirk Weissenborn, Xiaohua Zhai, Thomas Unterthiner, Mostafa Dehghani, Matthias Minderer, Georg Heigold, Sylvain Gelly, Jakob Uszkoreit, and Neil Houlsby. An image is worth 16x16 words: Transformers for image recognition at scale, 2020. 7
- [16] Mark Everingham, Luc Gool, Christopher K. Williams, John Winn, and Andrew Zisserman. The pascal visual object classes (voc) challenge. *Int. J. Comput. Vision*, 88(2):303–338, jun 2010. 4
- [17] Be My Eyes. Be My Eyes: Our story. 2
- [18] Be My Eyes. Bringing sight to blind and low-vision people. <https://www.bemyeyes.com/>, 2020. (Accessed on 01/08/2020). 2, 4
- [19] Deng-Ping Fan, Ming-Ming Cheng, Yun Liu, Tao Li, and Ali Borji. Structure-measure: A new way to evaluate foreground maps. In *ICCV*, pages 4548–4557, 2017. 13
- [20] Deng-Ping Fan, Cheng Gong, Yang Cao, Bo Ren, Ming-Ming Cheng, and Ali Borji. Enhanced-alignment measure for binary foreground map evaluation. In *IJCAI*, pages 698–704, 2018. 13
- [21] American Federation for the Blind. Low vision optical devices. 1
- [22] Ashish Kumar Gupta, Ayan Seal, Mukesh Prasad, and Priyee Khanna. Salient object detection techniques in computer vision—a survey. *Entropy*, 22(10), 2020. 1, 2
- [23] Danna Gurari, Kun He, Bo Xiong, Jianming Zhang, Mehrnoosh Sameki, Suyog Dutt Jain, Stan Sclaroff, Margrit Betke, and Kristen Grauman. Predicting foreground object ambiguity and efficiently crowdsourcing the segmentation (s). *International Journal of Computer Vision*, 126(7):714–730, 2018. 2
- [24] Danna Gurari, Qing Li, Chi Lin, Yinan Zhao, Anhong Guo, Abigale Stangl, and Jeffrey P Bigham. Vizwiz-priv: A dataset for recognizing the presence and purpose of private visual information in images taken by blind people. In *Proceedings of the IEEE/CVF Conference on Computer Vision and Pattern Recognition*, pages 939–948, 2019. 1, 2
- [25] Danna Gurari, Yinan Zhao, Meng Zhang, and Nilavra Bhat-tacharya. Captioning images taken by people who are blind. In *European Conference on Computer Vision*, pages 417–434. Springer, 2020. 1, 2, 6, 8
- [26] Kaiming He, Xiangyu Zhang, Shaoqing Ren, and Jian Sun. Deep residual learning for image recognition, 2015. 7
- [27] iDentifi. identifi. <http://getidentifi.com/>, 2020. (Accessed on 01/08/2020). 2
- [28] Hernisa Kacorri, Kris M Kitani, Jeffrey P Bigham, and Chieko Asakawa. People with visual impairment training personal object recognizers: Feasibility and challenges. In *Proceedings of the 2017 CHI Conference on Human Factors in Computing Systems*, pages 5839–5849, 2017. 2
- [29] Yin Li, Xiaodi Hou, Christof Koch, James M. Rehg, and Alan L. Yuille. The secrets of salient object segmentation. In *2014 IEEE Conference on Computer Vision and Pattern Recognition*, pages 280–287, 2014. 4, 5, 6, 13
- [30] Nian Liu, Ni Zhang, Kaiyuan Wan, Ling Shao, and Junwei Han. Visual saliency transformer, 2021. 2, 4, 6, 7, 8, 14
- [31] Ze Liu, Yutong Lin, Yue Cao, Han Hu, Yixuan Wei, Zheng Zhang, Stephen Lin, and Baining Guo. Swin transformer: Hierarchical vision transformer using shifted windows, 2021. 7
- [32] LookTel. Looktel recognizer. 1, 2
- [33] Mingcan Ma, Changqun Xia, and Jia Li. Pyramidal feature shrinking for salient object detection. *Proceedings of the AAAI Conference on Artificial Intelligence*, 35(3):2311–2318, May 2021. 2, 4, 6, 7, 8, 14
- [34] MDN. Fill-rule - svg: Scalable vector graphics: Mdn. 10

- [35] Federico Perazzi, Philipp Krähenbühl, Yael Pritch, and Alexander Hornung. Saliency filters: Contrast based filtering for salient region detection. In *CVPR*, pages 733–740, 2012. 8, 12
- [36] Federico Perazzi, Jordi Pont-Tuset, Brian McWilliams, Luc Van Gool, Markus Gross, and Alexander Sorkine-Hornung. A benchmark dataset and evaluation methodology for video object segmentation. In *The IEEE Conference on Computer Vision and Pattern Recognition (CVPR)*, 2016. 4
- [37] Xuebin Qin, Hang Dai, Xiaobin Hu, Deng-Ping Fan, Ling Shao, and Luc Van Gool. Highly accurate dichotomous image segmentation, 2022. 7, 8, 14
- [38] Xuebin Qin, Deng-Ping Fan, Chenyang Huang, Cyril Digne, Zichen Zhang, Adrià Cabeza Sant’Anna, Albert Suàrez, Martin Jagersand, and Ling Shao. Boundary-aware segmentation network for mobile and web applications, 2021. 4, 6, 7, 8
- [39] Abigale J Stangl, Esha Kothari, Suyog D Jain, Tom Yeh, Kristen Grauman, and Danna Gurari. Browsewithme: An online clothes shopping assistant for people with visual impairments. In *Proceedings of the 20th International ACM SIGACCESS Conference on Computers and Accessibility*, pages 107–118, 2018. 1
- [40] TapTapSee. Taptapsee. 1, 2
- [41] Wang, Lijun, Lu, Huchuan, Wang, Yifan, Feng, Mengyang, Wang, Dong, Yin, Baocai, Ruan, and Xiang. Learning to detect salient objects with image-level supervision. In *CVPR*, 2017. 4, 5, 7, 13
- [42] Wenguan Wang, Shuyang Zhao, Jianbing Shen, Steven C. H. Hoi, and Ali Borji. Salient object detection with pyramid attention and salient edges. In *Proceedings of the IEEE/CVF Conference on Computer Vision and Pattern Recognition (CVPR)*, June 2019. 1, 2
- [43] Jun Wei, Shuhui Wang, and Qingming Huang. F3net: Fusion, feedback and focus for salient object detection, 2019. 2, 4, 6, 7, 8, 14
- [44] Chenxi Xie, Changqun Xia, Mingcan Ma, Zhirui Zhao, Xiaowu Chen, and Jia Li. Pyramid grafting network for one-stage high resolution saliency detection, 2022. 2, 4, 5, 6, 7, 8, 13
- [45] Qiong Yan, Li Xu, Jianping Shi, and Jiaya Jia. Hierarchical saliency detection. In *2013 IEEE Conference on Computer Vision and Pattern Recognition*, pages 1155–1162, 2013. 4, 5, 13
- [46] Yang, Chuan, Zhang, Lihe, Lu, Huchuan, Ruan, Xiang, Yang, and Ming-Hsuan. Saliency detection via graph-based manifold ranking. In *Computer Vision and Pattern Recognition (CVPR), 2013 IEEE Conference on*, pages 3166–3173. IEEE, 2013. 4, 5, 7, 13
- [47] Xiaoyu Zeng, Yanan Wang, Tai-Yin Chiu, Nilavra Bhattacharya, and Danna Gurari. Vision skills needed to answer visual questions. *Proceedings of the ACM on Human-Computer Interaction*, 4(CSCW2):1–31, 2020. 2
- [48] Yi Zeng, Pingping Zhang, Jianming Zhang, Zhe Lin, and Huchuan Lu. Towards high-resolution salient object detection. In *Proceedings of the IEEE/CVF International Conference on Computer Vision*, pages 7234–7243, 2019. 4, 5, 7, 13

Appendix

This document supplements the main paper with additional information concerning:

1. Dataset Creation (supplements Section 3.1)
 - Annotation Task Interface
 - Worker Qualification Task
 - Analysis of Workers’ Annotation Differences
2. Dataset Analysis: VizWiz-SO vs Existing Datasets (supplements Section 3.2.2)
3. Experimental Design (supplements Section 4.1)

A. Dataset Creation

A.1. Annotation Task Interface

The task interface displays five images within a tabbed container on the left and preliminary questions with task instructions on the right. A screenshot of the task interface (without instructions) is shown in Figure 4.

To account for occlusions and holes while keeping the task simple for annotators, we permitted annotators to generate multiple polygons. For occlusions, annotators could use as many polygons as necessary for demarcating foreground objects partitioned into multiple polygons. For holes, we apply an even-odd fill rule to images featuring foreground objects with holes. With an even-odd fill rule, every area inside an even number of enclosed areas becomes hollow, and every region inside an odd number of enclosed areas becomes filled [34]. By treating the image’s four corners as the first enclosed area, the outermost boundary of the foreground object becomes the second enclosed area. Moreover, holes within foreground objects represent the third layer of enclosed areas and become filled, allowing annotators to demarcate foreground objects featuring holes. In practice, annotators first trace the outermost boundary of the foreground object and close the path by clicking the first point a second time. We then instructed annotators to trace any holes within the foreground object, and so those holes end up in odd-numbered layers.

A.2. Worker Qualification Task

We administered a qualification task for workers to support our collection of high-quality ground truth annotations. The qualification task required annotating five images, each of which features a distinct challenging annotation scenario. All five images are shown in Figure 5. The first two images show a table and a bench, offering examples with complex boundaries and holes. The next two images feature a person holding a coffee mug, to support educating a crowd-worker about our expectations for annotating objects with

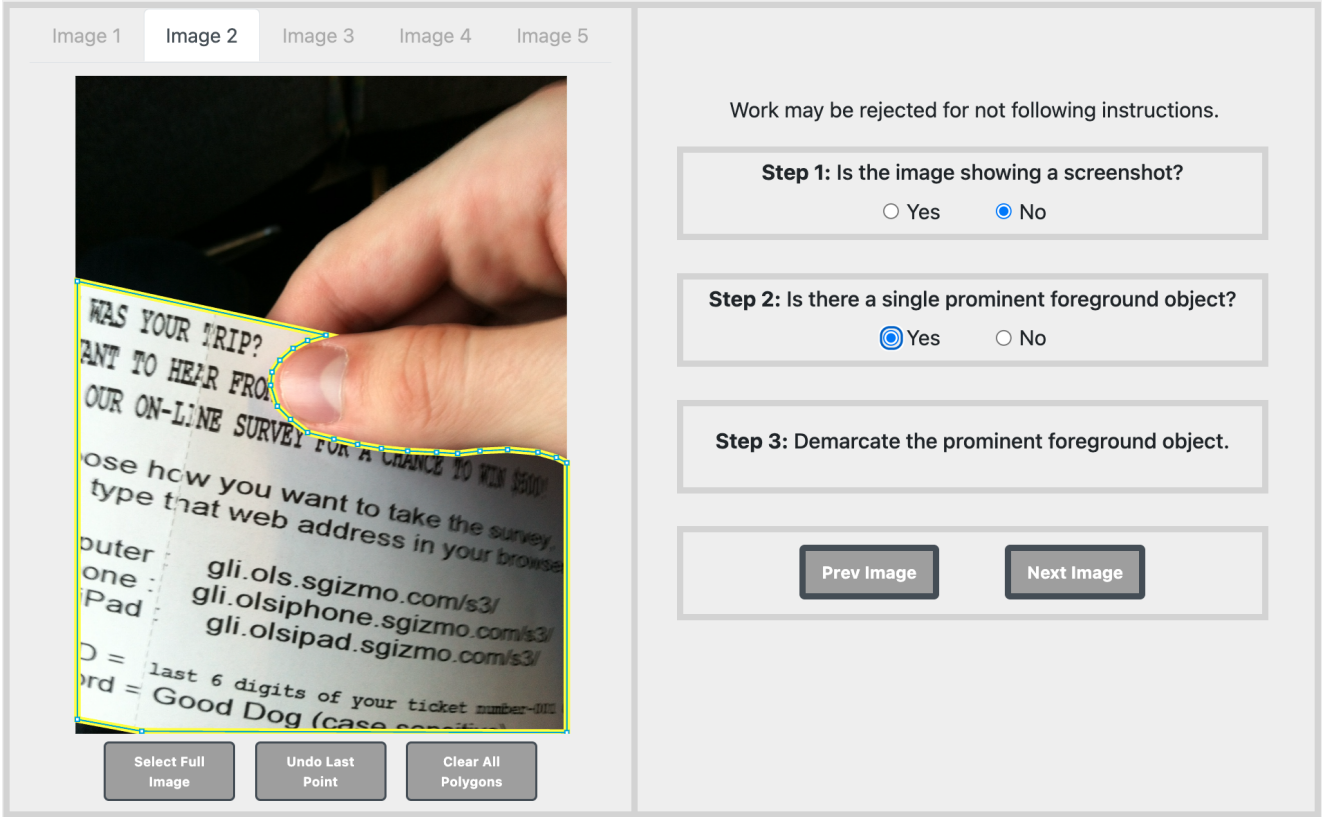


Figure 4. A screenshot of our annotation task interface.



Figure 5. The five images used for the worker qualification task. Each was selected to demonstrate a challenging annotation scenario such as complex boundaries, holes, and occlusions.

complex geometries that have many curves and occlusions that require annotating multiple polygons. The final image is a spatula. This task verified a crowdworker’s ability to correctly identify and annotate multiple holes that can arise within the salient object.

After crowdworkers annotated each qualification image, the backend code of our website checked if their annotation was sufficiently similar to the GT annotation (i.e., IoU similarity of at least 0.90). Crowdworkers could only proceed to the following image after they obtained an $\text{IoU} \geq 0.90$ on the current image. Crowdworkers obtaining an $\text{IoU} \geq 0.90$ on all five qualification assessment images on a per-image basis gave us substantial confidence that they would

be able to successfully handle complex and challenging outlier cases within the original VizWiz Dataset.⁷

A.3. Analysis of Workers’ Annotation Differences

We collected a larger number of redundant annotations per image for a random subset of images to better explore when and why annotation differences are observed from different workers. Specifically, for this analysis, we collected four annotations as opposed to two for a subset of 1,237 images. Examples of the redundant annotations collected per image are shown in Figure 6.

The first example (i.e., row 1 of Figure 6) highlights that annotation differences can stem from challenging annotation scenarios where objects contain holes (e.g., in mug handle) or are occluded (e.g., by the straw). For instance, the hole was not annotated in the third annotation. Additionally, only the fourth annotation captured the occlusion that arises from the straw.

The second example (i.e., row 2 of Figure 6) highlights that annotation differences can stem from ambiguity regard-

⁷Some crowdworkers did not pass the qualification assessment due to time constraints. In these cases, crowdworkers would contact us with the images they annotated. If we were confident in their annotation abilities, we manually added these crowdworkers to the qualified worker pool.

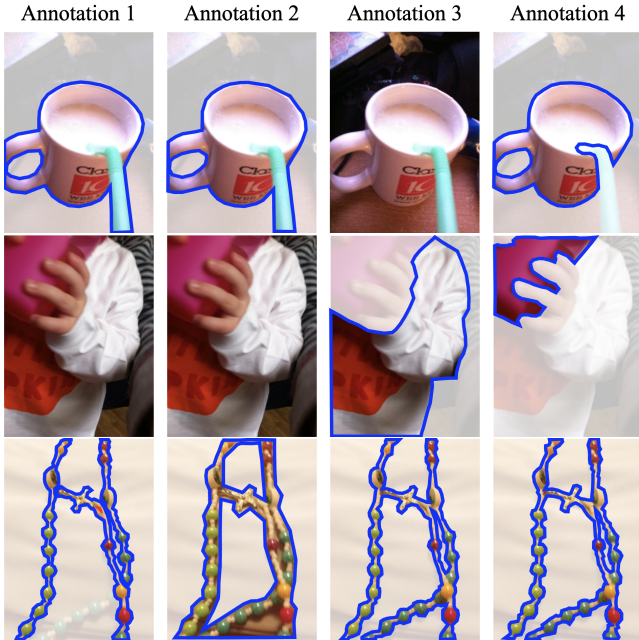


Figure 6. Example annotations from our random subset where we collected four annotations as opposed to two. We find worker differences primarily occur in challenging annotation scenarios such as holes, occlusions, complex boundaries, and object saliency.

ing what is the salient object. As shown, the first two annotations flag the image as lacking a foreground object, the third annotation identifies the child holding the cup as the salient object, and the fourth annotation identified the child’s cup as the salient object.

The third example (i.e., in row 3 of Figure 6) highlights that annotation differences also can arise for objects that simultaneously have complex boundaries and holes. In annotation one, the worker did not fully annotate the salient object, cutting out part of the object from the annotation. Only the third and fourth annotations accurately annotate all holes that are present in the salient object’s boundary while also having tight boundaries in the annotation.

In summary, we found occlusions, holes, and saliency ambiguity to be the primary factors contributing to annotation differences. In the case of occlusions, worker differences can arise when deciding whether to include objects that are a composite part of the salient object. In the case of holes, annotation differences can arise regarding which holes to annotate. Last, we found that it can be ambiguous as to which object is the most salient.

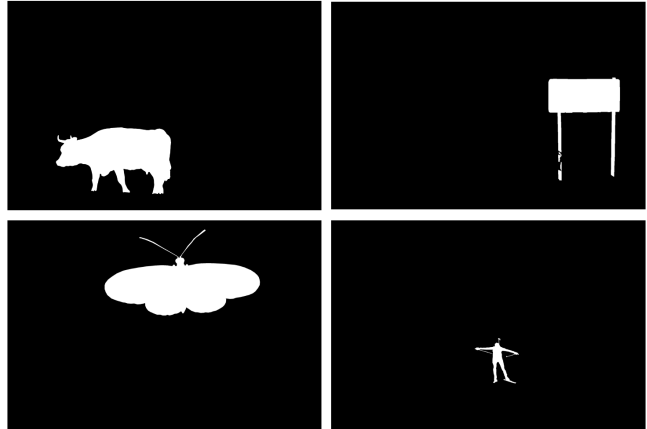


Figure 7. Example ground truth annotations from the HRSOD dataset which exemplify that salient objects are not usually not centered in the image. This is a common trend in the dataset.

B. Dataset Analysis

B.1. VizWiz-SO vs Existing Datasets

We present finer-grained details about typical image resolutions for the different salient object detection datasets to expand upon discussions in the main paper about how VizWiz-SO relates to other datasets. Specifically, we report the median image width (Med. W), median image height (Med. H), and whether the dataset supports high resolution images (High Res.) as defined by whether the median image height and width are greater than 1080 and 1920 respectively. Results are reported in Table 4. We observe that our new dataset, overall, provides higher resolution images than most datasets.

We also expand on a surprising finding reported in our main paper that the HRSOD dataset is the only one for which salient objects do not occupy the typical center positions. To do so, we visualize the ground truth masks of some non-centered objects in Figure 7. In row one, we see that objects are horizontally distributed to left and right positions of the images. Similarly, we observe in row two that the salient objects are vertically distributed to the top and bottom positions of the images.

C. Algorithmic Benchmarking

C.1. Experimental Design

We compute the five metrics used in the benchmarking section using the following definitions:

Mean Absolute Error [35] represents the average absolute difference between the predicted saliency map and its

	DAVIS-S [48]	PASCAL-S [29]	HR [48]	ECSSD [45]	DUT-O [46]	UH [44]	DUTS [41]	Ours
Med. W	1080	375	2704	300	300	3612	300	1296
Med. H	1920	500	3264	400	400	5000	400	968
High Res.	✓	✗	✓	✗	✗	✓	✗	✓

Table 4. Characterization of our VizWiz-SO dataset and seven existing salient object detection datasets with respect to metrics showcasing the image resolution. This includes median image width (“Med. W”), median image height (“Med. H”), and flag indicating if high resolution (“High Res.”). (HR=HRSOD; UH=UHRSD)

ground truth per pixel. It can be given as:

$$MAE = \frac{1}{H * W} \sum_{r=1}^H \sum_{c=1}^W |pred(r, c) - gt(r, c)| \quad (1)$$

where $pred$ represents the predicted saliency map, gt represents the ground truth, (H, W) represents the height and width of the image, and (r, c) represents the pixel coordinates for the given image.

Structure Measure [19] is used to measure the similarity between the predicted saliency map and the ground truth. Since, we convert both the predictions and ground truths into the $[0, 1]$ range, we apply the formula directly to the predictions and maps. It can be defined as follows:

$$S_m = (1 - \alpha)S_r + \alpha S_o \quad (2)$$

where, S_r is defined as the region aware similarity score, S_o is defined as the object aware similarity score, and α represents the weight that is used to sum up the values. We set $\alpha = 0.5$, therefore making sure that we see equal contribution from both region and object aware scores.

F-Measure [2] represents the precision and recall ratio for the given prediction. It can be represented as:

$$F_m = \frac{(1 + \beta^2) * Precision * Recall}{\beta^2 * Precision + Recall} \quad (3)$$

Here $precision = \frac{TP}{TP+FP}$ and $recall = \frac{TP}{TP+FN}$ on the entire prediction image by pixels. We set $\beta^2 = 0.3$ and report the average of all F-measures as F_m similar to previous works.

Enhanced Alignment Measure [20] is used as the metric to measure the effectiveness of the saliency prediction against the ground truth. It captures the pixel-level matching information and image-level statistics into one single metric by the means of an enhanced alignment matrix ϕ . It is defined as follows:

$$E_m = \frac{1}{H * W} \sum_{r=1}^H \sum_{c=1}^W \phi_{FM}(r, c) \quad (4)$$

where, ϕ_{FM} represents the enhanced alignment matrix for the foreground map, (H, W) represents the height and

width of the image, and (r, c) represents the pixel coordinates for the given image.

Intersection over Union also known as Jaccard Index is used to determine the similarity between sample sets. In this case it captures the overlap between the ground truth and prediction map of the salient object. We convert the predictions in binary map and compute the Jaccard Index over two classes. It can be defined as follows:

$$IoU = J(A, B) = \frac{|A \cap B|}{|A \cup B|} \quad (5)$$

where, A and B are images of same size, consisting of integer class values $\{0, 1\}$.

We further show how the models performed on VizWiz-SO with qualitative examples shown in Figure 8. These examples feature a variety of challenges we observed for the models, such as a large salient object, less complex boundaries, lack of text on the salient object, and lower quality images. For example, we observe how the models fail to perform adequately in identifying larger salient objects (rows 4 and 5). We also observe the models perform better when salient objects contain text (rows 1 and 2) versus lack text (rows 5 and 6). Further, we see models perform worse for images that are lower quality (rows 3, 4, and 5). Our fine-grained analysis in the main paper suggests each of these factors offer unique challenges for modern salient object detection models.

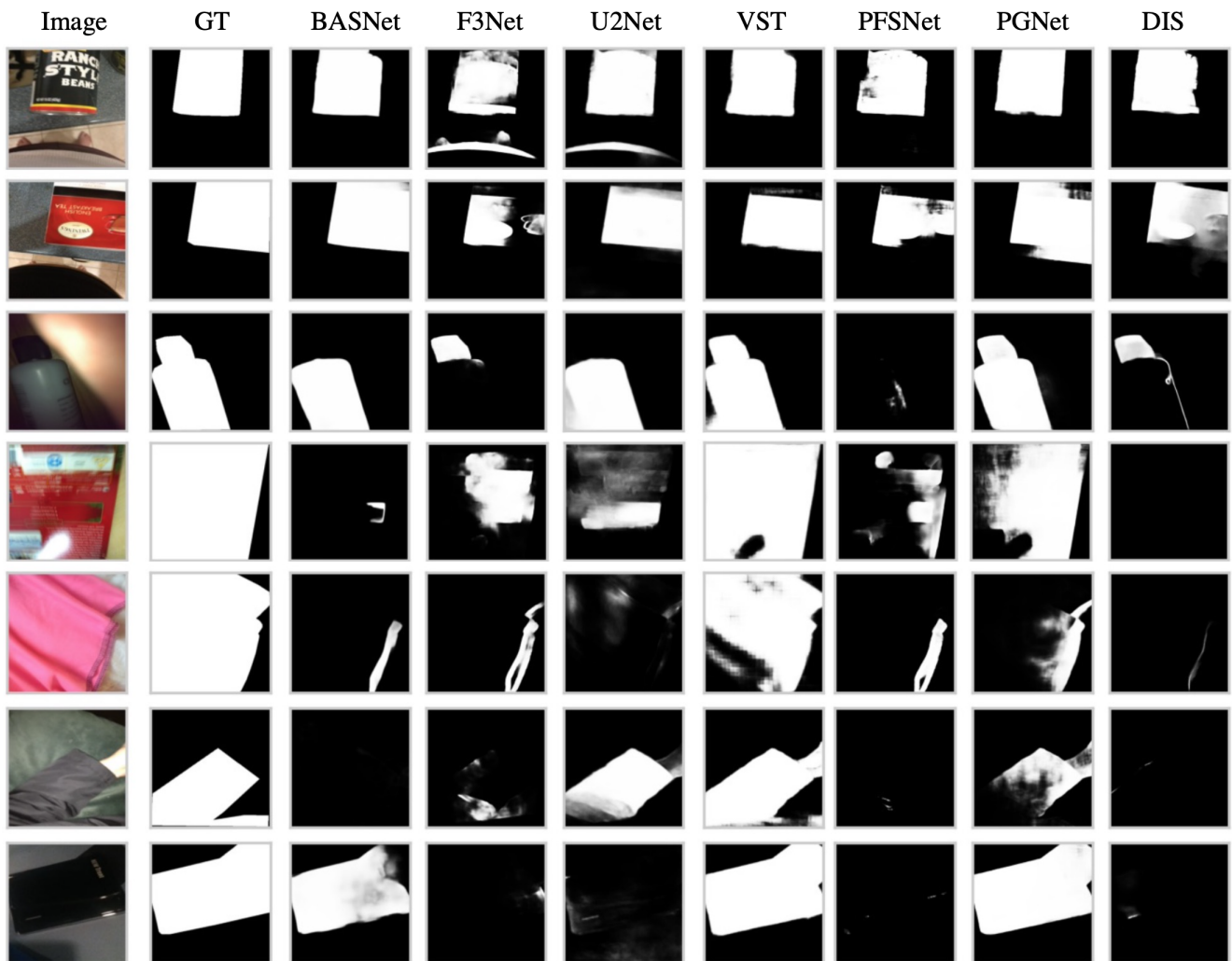


Figure 8. Examples of difficult images present in VizWiz-SO, with characteristics such as high coverage ratio, presence of text, less complex boundaries, and lower image quality. We show how the seven models perform on these cases as compared to the human annotation (GT=Ground Truth). We see that models such as PFSNet [33], DIS [37], and F3Net [43] do not always give us the correct salient objects or sometime no predictions at all. We also notice that VST [30] usually predicts salient objects with better accuracy compared to other models, but also suffer from not detecting the correct salient object.